Adsorption (2015) 21:53–65
DOI 10.1007/s10450-015-9649-9

Adsorption isotherms and kinetics of carbon dioxide on Chinese dry coal over a wide pressure range

Yongchen Song · Wanli Xing · Yi Zhang · Weiwei Jian · Zhaoyan Liu · Shuyang Liu

Received: 23 May 2014 / Revised: 13 September 2014 / Accepted: 12 January 2015 / Published online: 22 January 2015

Abstract A gravimetric method with in situ density measurement is used to determine the adsorption isotherms and kinetic characteristics of CO_2 on Chinese dry coal plug at 293.29, 311.11, 332.79 and 352.57 K and pressures up to 19 MPa. The adsorption and desorption process is reversible, which shows that it is a process of physical adsorption for CO_2 on coal. The excess adsorption increases with the increasing pressure at low pressures until the CO_2 phase transitions pressure is reached. Above this pressure, the excess adsorption decreases with the increasing pressure. The adsorption behaviour is described using the CO_2 density instead of pressure in four thermodynamic models such as modified Langmuir, Langmuir + k, DR and DR + k. It is found that the modified Langmuir + k and DR + k models are more suitable for liquid and supercritical CO_2 adsorption, respectively. The adsorption kinetics data are also obtained during the measurement of adsorption isotherms. The experimental data are fluctuant at the initial time range due to the temperature variation in the adsorption cell after high-pressure CO_2 is injected. The diffusivity is estimated using a modified unipore model. It is observed that the kinetic parameter C, accounting for the effect of gas diffusivity, increases with the increasing pressure at low pressures and has no obvious relations with pressure at high pressures. In this study, C value has no dependencies with temperature for CO_2, and the order of magnitude of the effective diffusivity is approximately 10^{-5} to 10^{-4} s^{-1}.

Y. Song · W. Xing · Y. Zhang (✉) · W. Jian · Z. Liu · S. Liu
Key Laboratory of Ocean Energy Utilization and Energy Conservation of Ministry of Education, School of Energy and Power Engineering, Dalian University of Technology, Dalian 116024, People's Republic of China
e-mail: zhangyi80@dlut.edu.cn

Keywords Adsorption isotherms · Thermodynamic model · Kinetics · Diffusivity

1 Introduction

It is generally known that the main contributor to climate change is the anthropogenic emission of carbon dioxide. Carbon dioxide capture and storage (CCS) technologies have been proposed to reduce the CO_2 concentration in the atmosphere. Among them, CO_2 sequestration in unminable coal seams has become a promising approach because the adsorption capacity of CO_2 is larger than that of methane on coal. China is a country with prominent coal production and consumption in which a storage capacity of 9.88×10^9 t CO_2 can be buried, and 4.26×10^{12} m^3 additional coal bed methane can be recovered by CO_2 injection (Fang and Li 2014). Consequently, based on the environmental and economic benefit of CO_2-ECBM (Enhanced Coal Bed Methane), there is a growing demand for a better understanding of CO_2 adsorption and transport on coal.

In general, the geological coal seams for CO_2 injection cover broad temperature (288–353 K) and pressure ranges (5–20 MPa) at a burial depth between 500 and 2000 m. The CO_2 adsorption on various coals at subcritical pressures have been introduced in the review of Siemons and Busch (2007), the CO_2 excess adsorption on dry coal increased with the increasing pressure. However, some results with respect to the isotherms were controversial at supercritical pressures. Toribio et al. (2004) proposed that the adsorption capacity of CO_2 on Japanese dry coal increased continually beyond the critical point when the measurements were performed up to 15 MPa at 308, 318 and 328 K. However, the isotherms of CO_2 adsorption on dry coal showed a nonlinear decrease under supercritical

conditions (Bae and Bhatia 2006; Ottiger et al. 2006; Sakurovs et al. 2007). The conclusion was similar to that of Humayun and Tomasko (2000) with regard to CO_2 adsorption on activated carbon at pressures up to 20 MPa at (313–333) K. The maximum excess adsorption of CO_2 on dry coal appeared between 8 and 10 MPa (Siemons and Busch 2007; Krooss et al. 2002). Besides, research regarding the isotherm of liquid CO_2 on coal is scarce. Therefore, it is necessary to accurately measure the adsorption behaviour of liquid and supercritical CO_2 on coal.

To describe the adsorption behaviour of CO_2 on coal, conventional adsorption isotherm models have been proposed such as the Langmuir monolayer model, the Dubinin (DR and DA) pore-filling model, and the BET multi-layer model. Among these models, the accuracy of Dubinin's model is higher than that of the Langmuir model for CO_2 at low pressures (Harpalani et al. 2006; Dutta et al. 2008). Extensions of the aforementioned approaches were introduced to provide the best fit to experimental data under supercritical conditions. The Langmuir and DR models were adequate for modeling supercritical CO_2 adsorption on coal when they were modified using the CO_2 density instead of pressure (Sakurovs et al. 2007, 2008, 2010). However, the CO_2 density needs to be calculated using an equation of state for a volumetric experiment system. In this work, gas density can be determined in situ in the experimental system of a magnetic suspension balance (MSB), and applied directly to the modified adsorption isotherm models.

Most kinetic measurements were performed for CO_2 under subcritical conditions, and the researches mainly focused on monitoring the rate of pressure equilibrium by using the volumetric and manometric methods (Busch et al. 2004; Bhowmik and Dutta 2013; Clarkson and Bustin 1999a, 1999b; Li et al. 2010; Pan et al. 2010; Siemons et al. 2007). Only a few adsorption kinetics data were published using the gravimetric method to determine the change of coal mass under supercritical conditions (Charrière et al. 2010; Kelemen and Kwiatek 2009). Meanwhile, the diffusivity of CO_2 in coal is often estimated by Fick's second law to interpret the adsorption and diffusion rate for spherical sorbent particles, for instance, the unipore and bidisperese models. However, the mathematical description of Fick's second law for coal-CO_2 systems was very difficult, so some improved models were proposed (Terzyk and Gauden 2001; Mianowski and Marecka 2009). Although those approaches can guarantee minimal error of estimation as the experimental data of the adsorption kinetics was fitted, they were commonly used at low pressures (less than 7.38 MPa). Correspondingly, there was less study on diffusivity for CO_2 in coal at high pressures, and the effects of pressure on diffusivity were inconsistent with each other in previous researches (Busch et al. 2004; Charrière et al. 2010; Nandi and Walker 1975; Cui et al. 2004).

In this study, the measurements for static and dynamic adsorption were conducted in a gravimetric adsorption system at 293.29, 311.11, 332.79 and 352.57 K and pressures up to 19 MPa. Then, four thermodynamic models were applied to depict the adsorption behaviour of CO_2 on coal. Finally, the diffusivity was estimated from adsorption kinetics data with a modified unipore model.

2 Experimental section

2.1 Materials

There are a few studies on coal plugs instead of small coal particles (Day et al. 2008; Hol et al. 2013; Kelemen and Kwiatek 2009; Majewska and Ziętek 2007; St. George and Barakat 2001). But most studies focus on the low pressure region in the literatures, and few dynamic adsorption experiments on block coal are performed in the gravimetric system. To maintain the matrix and cleat systems of block coal consistency with the coal reservoir, fresh coal blocks were taken from the Datong coal mine located in the Shanxi province of China in this study. According to the shape of the adsorption cell in MSB, the coal sample was processed into a hollow cylinder with inner and outer diameters of 6.4 and 16 mm, respectively, and a length of 15 mm. Physical properties of the raw coal in the experiments were listed in Table 1. In this work, the organic petrographic analysis suggests that vitrinite matter is the most abundant maceral, followed by inertinite and mineral matter. The average value of maximum vitrinite reflectance ($R_{o,max}$) is 3.72 %, which indicates that the coal sample is typical anthracite. The microstructural study was performed on the coal sample using scanning electron microscopy (SEM) with 200 and 1000 magnification, as shown in Fig. 1. SEM observations reveal that hollow particles in the coal sample appear to such roughness of the surface, which is favourable to increase the interspace among particles and to retain adsorption amount on the coal surface.

Additionally, the coal sample should be degassed before the adsorption experiments. In this study, the coal sample was dried in the MSB at 378 K under vacuum for 12 h to remove the physically adsorbed moisture without altering the adsorbent structure (Bae and Bhatia 2006; Ottiger et al. 2006; Charrière et al. 2010; Miknis et al. 1996; Romanov and Soong 2009).

The gases used in this study such as CO_2, N_2, and He were obtained from Dalian Da-te Gas Co., Ltd. with a purity of 99.99, 99.999 and 99.999 %, respectively.

Table 1 Physical properties of the raw coal used in the experiment

Proximate analysis (wt% ad)		Ultimate analysis (wt% ad)		Petrographic analysis (vol.%, mmf)	
Ash	37.48	Carbon	50.730	Vitrinite	73.00
Moisture	0.86	Hydrogen	2.169	Liptinite	0.00
Volatile matter	10.48	Nitrogen	35.630	Inertinite	16.20
Fixed carbon	51.18	Oxygen	7.653	Mineral	10.80
		Sulfur	0.927	$R_{o'max}$	3.72

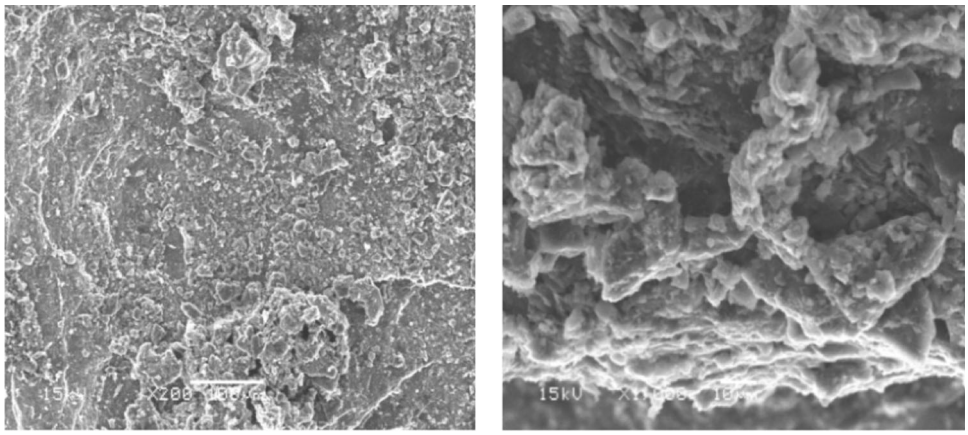

×200 ×1000

Fig. 1 Microstructure of the coal sample with SEM

2.2 Experimental apparatus

The adsorption experiments were performed using a gravimetric adsorption system, which consists of a MSB, a data acquisition system, a thermostatic system, a gas supply system, and a vacuum pump. The MSB can be operated with an absolute accuracy of 10^{-5} g at temperatures ranging from 253 K to 523 K and pressures up to 20 MPa. The schematic diagram of the system is shown in Fig. 2. The MSB is composed of a measuring cell, an electromagnet, a permanent magnet, and a microbalance. The measuring cell is filled with CO_2, whose density can be measured by the titanium sinker. The coal sample is located in the adsorption cell. The temperature in the measuring cell is controlled by a JULABO FP 50-ME Refrigerated/Heating Circulator and measured with a Pt100 temperature sensor whose accuracy is ± 0.01 K. The pressure is measured by a pressure probe (20 MPa, reproducibility 0.08 %) connecting the gas tube with a T-piece.

2.3 Experimental principle

The gravimetric adsorption system allows the measurement of the weight change of the coal sample and gas density simultaneously, of which basic principle is buoyancy effect. The forces acted on the adsorption cell and coal sample are illustrated in Fig. 2, where F_1, F_2, and G are the values determined by MSB at the experimental conditions, the buoyancy induced by the free fluid, and the gravity of adsorption cell and coal sample, respectively. The buoyancy effect for MSB has been described extensively elsewhere (Dreisbach et al. 2002; Pini et al. 2006; Ottiger et al. 2008; Song et al. 2012).

$$F_1 + F_2 = G \tag{1}$$

$$m'\left(\rho_{CO_2}, T\right)g + \rho_{CO_2}(P,T)\left(V_{sc} + V_{ads} + V_{swelling}\right)g = m\left(\rho_{CO_2}, T\right)g \tag{2}$$

where m' (ρ_{CO_2}, T) is the apparent mass of adsorption cell, coal sample and adsorbed phase obtained by MSB when CO_2 is injected in measuring cell at temperature T; g is the gravitational acceleration; $\rho_{CO_2}(P,T)$ is CO_2 density measured by MSB at pressure P and temperature T; V_{sc} is the volume of adsorption cell and coal sample; V_{ads} is the volume of adsorbed phase; $m(\rho_{CO_2},T)$ is the mass of adsorption cell, coal sample and adsorbed phase; $V_{swelling}$ is the swelling volume of the coal sample induced by the adsorbed CO_2.

It's proposed that the swelling has little effect on the adsorption isotherm data for high rank coal such as anthracite (Ozdemir et al. 2003, 2004). In this work, the adsorption experiments are performed for CO_2 on the block coal sample, which is typical anthracite. As a kind of high rank coal, the swelling volume of the coal induced by CO_2 adsorption in the calculation can be neglected.

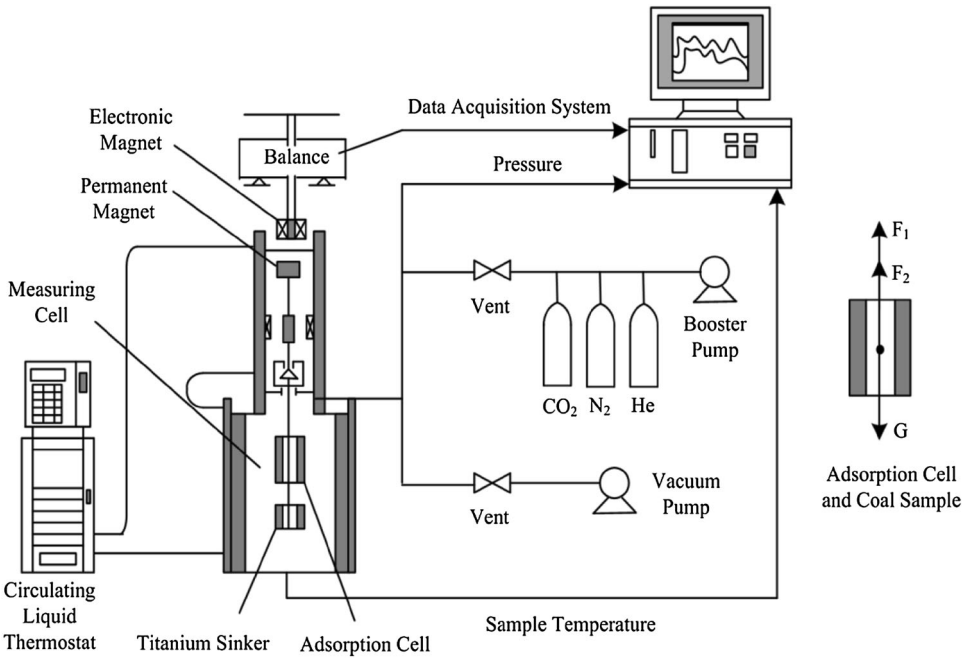

Fig. 2 Set-up for gravimetric measurement of the adsorption equilibrium of CO_2

2.4 Excess adsorption measurements

The measuring cell was evacuated prior to the gas injection. The CO_2 was injected into the measuring cell after coal sample was placed and degassed in the adsorption cell. The adsorption measurement was performed at the desired temperature and pressure conditions. The CO_2 density ($\rho_{CO_2}(P,T)$) and the apparent mass of adsorption cell, coal sample and adsorbed phase ($m'(\rho_{CO_2},T)$) can be obtained in situ until the adsorption equilibrium is reached when the mass of coal sample remains constant within 720 s and the fluctuation tolerance of pressure is about 0.0003 MPa/min for the pressure transducer. Then, these data were used to calculate the excess adsorption mass ($m_{CO_2}(P,T)$), as shown in Eq. 3. In this study, the swelling volume of block coal sample is neglected.

$$\begin{aligned} m_{CO_2}(P,T) &= m\left(\rho_{CO_2},T\right) - m_{sc} - \rho_{CO_2}(P,T)V_{ads} \\ &= m'\left(\rho_{CO_2},T\right) - m_{sc} + \rho_{CO_2}(P,T)V_{sc} \end{aligned} \quad (3)$$

where $m_{CO_2}(P,T)$ is the excess adsorption mass of CO_2 on dry coal at pressure P and temperature T; m_{sc} is the mass of adsorption cell and coal sample.

The unknown parameters in Eq. 3 include m_{sc} and V_{sc}, which can be measured as follows.

2.4.1 Mass of adsorption cell

To obtain the mass and volume of the blank adsorption cell, this measurement was performed only once by injecting nitrogen into the measuring cell up to 10 MPa at 292.72 K. Owing to the existence of nitrogen, the blank adsorption cell is subject to downward gravity and upward buoyancy. Therefore, the mass of the adsorption cell in a vacuum (m_s) is obtained by the apparent weight of the adsorption cell ($m'_s(\rho_{N_2},T)$) measured by MSB and the buoyancy of the adsorption cell induced by N_2 at different pressures. This measurement is expressed as Eq. 4, where the relationship between ($m'_s(\rho_{N_2},T)$) and $\rho_{N_2}(P,T)$ is linear, as shown in Fig. 3. Therefore, the mass (m_s) and volume (V_s) of the blank adsorption cell can be obtained by using the least square method. Namely, the y-axis intercept and the absolute value of the slope are considered as m_s and V_s, which are 6.1035 g and 0.7767 cm^3, respectively.

$$m'_s\left(\rho_{N_2},T\right) = m_s - \rho_{N_2}(P,T)V_s \quad (4)$$

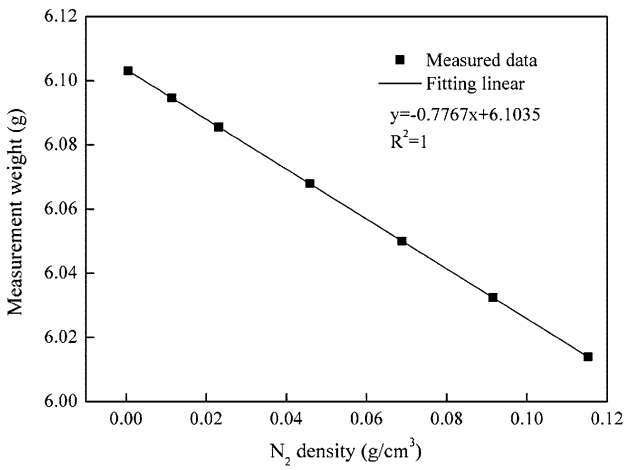

Fig. 3 Measurement of the blank adsorption cell with N_2 at 292.72 K

where $\rho_{N_2}(P,T)$ is the density of nitrogen at experimental pressure P and temperature T.

2.4.2 Mass and volume of adsorption cell and coal sample

Helium was injected into the measuring cell after coal sample was placed in the adsorption cell, and then the total mass and volume of the adsorption cell and coal sample can be determined. Although the adsorption capacity of helium is very small, it can still be affected by the experimental temperature and pressure (Ottiger et al. 2006; Charrière et al. 2010). In addition, the texture and density of dry coal might change when exposed to helium up to 7 MPa at room temperature (Romanov and Soong 2009). Consequently, the measurements of the mass and volume of the adsorption cell and coal sample were performed at 378 K up to 5.3 MPa in this study. The forces acted on the adsorption cell and coal sample were similar to the blank adsorption cell, as indicated in Eq. 5. Using the same method, the mass (m_{sc}) and volume (V_{sc}) of the adsorption cell and coal sample are 10.6919 g and 3.0807 cm^3, respectively.

$$m'_{sc}(\rho_{He},T) = m_{sc} - \rho_{He}(P,T)V_{sc} \quad (5)$$

where $m'_{sc}(\rho_{He},T)$ is the apparent mass of the adsorption cell and coal sample; $\rho_{He}(P,T)$ is the density of helium at experimental pressure P and temperature T, both of which can be determined by MSB. The measured helium densities in the experiment are given in Table 2, which shows that the measured helium densities can achieve the accuracy of 0.00003 g/cm^3.

After this measurement, the mass of the coal sample (m_c) can be obtained by Eq. 6.

$$m_c = m_{sc} - m_s \quad (6)$$

In conclusion, the molar excess adsorption (n_{ex}) defined as the per unit mass of coal can be expressed by Eq. 7 at a given pressure P and temperature T.

$$n_{ex} = \frac{m_{CO_2}(P,T)}{M_{CO_2}m_c} \quad (7)$$

Table 2 Specification of the experimental parameters for He measurement at 378 K

P (MPa)	ρ_m (g/cm^3)	ρ_{NIST} (g/cm^3)	AE (g/cm^3)
2.25	0.00287	0.00285	0.00002
3.66	0.00463	0.00460	0.00003
4.56	0.00572	0.00571	0.00001
5.24	0.00655	0.00655	0.00000

Remarks: ρ_m is the He density measured by experiment; ρ_{NIST} is the He density obtained by the National Institute of Standards and Technology (NIST); AE is the absolute error, AE = $|\rho_m - \rho_{NIST}|$

where m_{CO_2} is the molar mass of CO_2.

This process is repeated at given pressure intervals until the maximum pre-selected pressure is reached. Each of the resulting equilibrium pressure is then plotted to provide an isotherm. The desorption process of CO_2 on coal was performed by depressurisation after the adsorption experiment. The adsorption kinetics data can be obtained by monitoring the mass changes of the coal sample and CO_2 density with time during the isothermal adsorption experiments.

3 Results and discussion

The adsorption and desorption isotherms and the kinetic characteristics of carbon dioxide on Chinese dry coal were determined using the magnetic suspension balance at 293.29, 311.11, 332.79 and 352.57 K and pressures up to 19 MPa.

3.1 Reproducibility tests

Two independent runs for the same block coal sample were performed to confirm the reproducibility of the data at 311.11 K, as shown in Fig. 4. The results show that the two runs are in good agreement, which verify the reproducibility of our experimental system.

3.2 Uncertainty in the excess adsorption

Potential sources of experimental errors and uncertainties have been discussed in the coal research community (Gensterblum et al. 2010; Hol et al. 2013; Mohammad et al. 2009; van Hemert et al. 2009). The uncertainties in

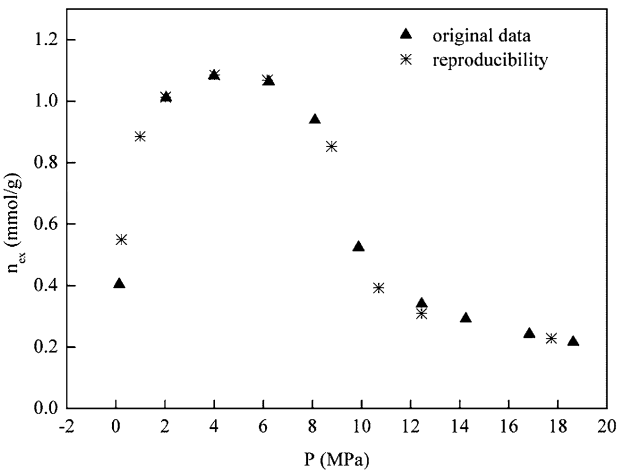

Fig. 4 Reproducibility test of the excess adsorption isotherms for CO_2 on dry coal at 311.11 K

the molar excess adsorption (u_{nex}) and the mass excess adsorption ($u_{m_{\mathrm{CO_2}}(P,T)}$) on the basis of Eqs. 3 and 7 are given as:

$$u_{n_{ex}} = \sqrt{\left(\frac{\partial n_{ex}}{\partial m_{sc}}\right)^2 u_{m_{sc}}^2 + \left(\frac{\partial n_{ex}}{\partial m_s}\right)^2 u_{m_s}^2 + \left(\frac{\partial n_{ex}}{\partial m_{\mathrm{CO_2}}(P,T)}\right)^2 u_{m_{\mathrm{CO_2}}(P,T)}^2} \tag{8}$$

$$u_{m_{\mathrm{CO_2}}(P,T)} = \sqrt{u_{m'\left(\rho_{\mathrm{CO_2}},T\right)}^2 + u_{m_{sc}}^2 + \left(\frac{\partial m_{\mathrm{CO_2}}(P,T)}{\partial \rho_{\mathrm{CO_2}}(P,T)}\right)^2 u_{\rho_{\mathrm{CO_2}}(P,T)}^2 + \left(\frac{\partial m_{\mathrm{CO_2}}(P,T)}{\partial V_{sc}}\right)^2 u_{V_{sc}}^2} \tag{9}$$

where u is the standard uncertainty.

The uncertainties caused by m_{sc}, m_{s} and V_{sc} can be obtained using generalized least squares, the results of u_{msc}, u_{ms}, and u_{Vsc} are 0.000359 g, 0.000034 g and 0.069938 cm^3, respectively. Based on the buoyancy effect of density measured by MSB in Song et al. (Song et al. 2012) and the volume correction of titanium sinker mentioned by Zhang et al. (Zhang et al. 2011), the uncertainty for measured density of CO_2 is calculated as:

$$u_{\rho_{\mathrm{CO_2}}(P,T)} = \sqrt{\left(\frac{\partial \rho_{\mathrm{CO_2}}(P,T)}{\partial m'\left(\rho_{\mathrm{CO_2}},T\right)}\right)^2 u_{m'\left(\rho_{\mathrm{CO_2}},T\right)}^2 + \left(\frac{\partial \rho_{\mathrm{CO_2}}(P,T)}{\partial V(P,T)}\right)^2 u_{V(P,T)}^2 + \left(\frac{\partial \rho_{CO_2}(P,T)}{\partial m_{cal}}\right)^2 u_{m_{cal}}^2} \tag{10}$$

where $V(P,T)$ is the correction volume of titanium sinker at experimental pressure P and temperature T; m_{cal} is the mass of titanium sinker in vacuum.

The excess adsorption capacity and the standard uncertainty at each pressure for CO_2 on the block coal sample have been listed in Table 5 in Appendix. The minimum and maximum of excess adsorption/desorption capacity are 0.10755 mmol/g and 1.18799 mmol/g, and the corresponding uncertainty are 0.000004 mmol/g and 0.00032 mmol/g, respectively. The percentage of standard uncertainty is from 0.004 % to 0.027 %.

3.3 Adsorption and desorption isotherms

The experimental data of the excess adsorption and desorption for CO_2 on the dry coal at 293.29, 311.11, 332.79 and 352.57 K are listed in Table 5 in Appendix. The adsorption data are connected by lines to guide the reader's eye in Fig. 5. The desorption isotherms are almost coincident with the adsorption isotherms at the same temperature. However, the differences between the adsorption and desorption capacities at approximately 0.1 MPa come from errors in CO_2 density measurement at low pressures. The reversible process of adsorption and desorption indicates that CO_2 adsorption on coal is a physical adsorption process. For lower pressures, the amount of excess adsorption increases with pressure, and the maxima become higher at a lower temperature. The maximum excess adsorption appeared near the phase transition pressure of CO_2 at 293.29 K, while it appeared near the critical pressure of CO_2 at 311.11, 332.79 and 352.57 K. Above this pressure, the excess adsorption amount shows a downward trend and the nonlinear drop becomes steeper and larger at lower temperature. The reasons on the shape of excess CO_2 isotherm at subcritical or supercritical temperature can be explained as: one is that the volume of the adsorbed phase has measurable effects for increasing buoyancy in gravimetric measurements at high pressures; the other is the

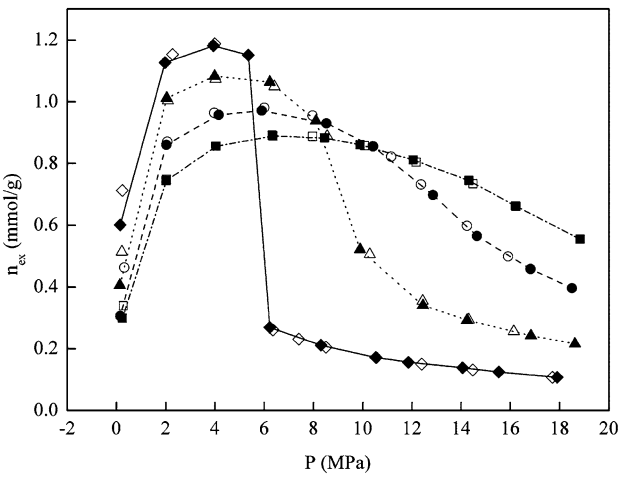

Fig. 5 Excess adsorption and desorption isotherms of CO_2 on dry coal, solid and open markers refer to adsorption and desorption, respectively. *Filled and open diamonds*, 293.29 K; *filled and open triangles*, 311.11 K; *filled and open circles*, 332.79 K; *filled and open squares*, 352.57 K

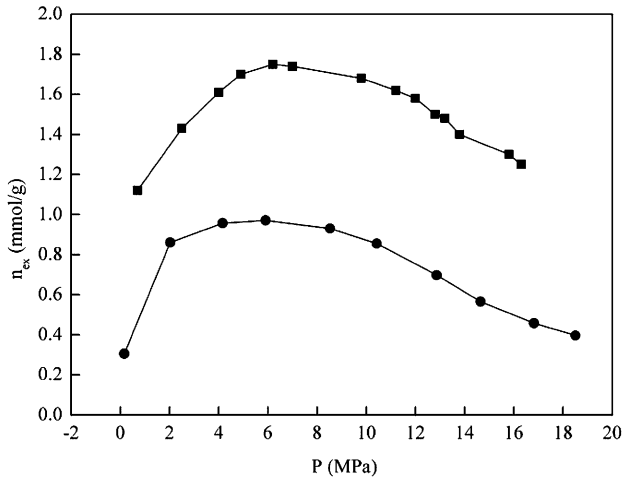

Fig. 6 Comparison of the excess adsorption isotherms reported in this work and literatures at 334 K. *Filled square*, crushed coal in Gensterblum et al. (2013); *filled circle*, block coal sample in this work

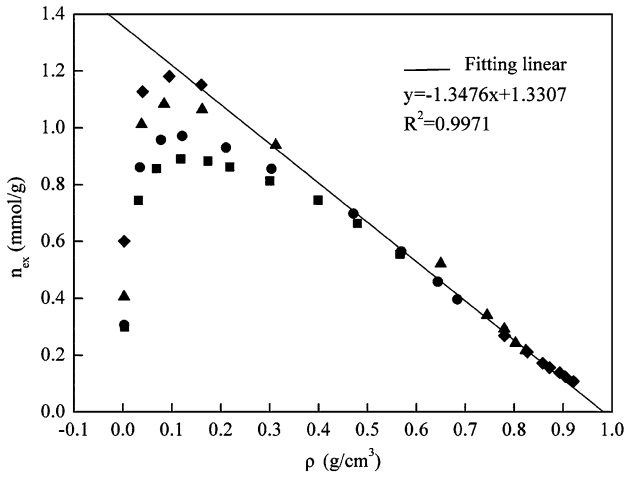

Fig. 7 Excess adsorption isotherms of CO_2 on dry coal plotted as a function of free CO_2 density. *Filled diamond*, 293.29 K; *filled triangle*, 311.11 K; *filled circle*, 332.79 K; *filled square*, 352.57 K

nonlinearity of the relationship between CO_2 density and pressure. Besides, it is also a result of the free CO_2 density approaching that of the adsorbed phase under supercritical conditions. Similar results were reported in some literatures for crushed anthracite (Siemons and Busch 2007; Gensterblum et al. 2013). As is known to all, supercritical CO_2 has higher diffusivity and lower viscosity compared to liquid CO_2, which would result in improved mass transfer properties during adsorption/desorption. So the excess adsorption capacity for supercritical CO_2 on coal is higher than that for liquid CO_2 at high pressures.

Moreover, compared with the isotherm reported for CO_2 adsorption on the anthracite (Gensterblum et al. 2013), the trend of pressure effect on excess adsorption is similar as shown in Fig. 6. The excess adsorption capacity for CO_2 on coal increases with pressure until maximum and then decreased at higher pressures. But the elemental composition and the micro-pore system of coal, especially the volume and specific surface in micro-pore system play a decisive role for adsorption properties, and they are positively related to adsorption capacity. So the excess adsorption on the crushed anthracite is apparently larger than that of block coal sample in this study due to the bigger pore volume and specific surface area for crushed coal.

The relationship between the amount of excess adsorption and CO_2 density is discussed in Fig. 7. It is clearly shown that the excess adsorption capacity increases up to the maximum in low density regions and then almost decreases linearly with the CO_2 density at different temperatures. The temperature has no obvious impact on the excess adsorption in high density ranges. In addition, the density of adsorbed phase cannot be measured directly, which was estimated by different methods in previous literatures (Sakurovs et al. 2007; Humayun and Tomasko 2000; Li et al. 2010; Sudibandriyo et al. 2003). If the adsorbed phase extends to a finite distance beyond the coal surface, then the adsorption amount of surface excess can be expressed in terms of the adsorbed phase density and volume as Eq. 11. In this study, an estimate from the excess adsorption isotherm was used, which is based on Eq. 11 and illustrated in Fig. 7.

$$n_0 = \rho_a V_{ads} - \rho_{CO_2}(P,T)V_{ads} \tag{11}$$

where n_0 is the adsorption amount of surface excess for CO_2 on coal; ρ_a is the density of adsorbed phase.

The linear relationship between n_0 and $\rho_{CO_2}(P,T)$ at high densities indicates that the density and volume of adsorbed phase become constant after a certain point. The slope and intercept would give the density and volume of the adsorbed phase, as shown in Fig. 7, where $\rho_a = 0.9874$ g/cm^3. It's worth noting that this method requires sufficient high-pressure data in the linear region beyond the maximum in the excess adsorption.

3.4 Adsorption thermodynamic model

The traditional Langmuir and DR models are widely used to predict the adsorption capacity of adsorbent at low pressures. The relationship between excess adsorption and pressure are expressed as Eqs. 12 and 13.

$$n_{ex} = n_0 P/(P + P_L) \quad \text{(traditional Langmuir model)} \tag{12}$$

$$n_{ex} = n_0 \exp\left\{-D[\ln(P_s/P)]^2\right\} \quad \text{(traditional DR model)} \tag{13}$$

where P is the pressure; P_L is the Langmuir pressure where half the adsorption sites are occupied; D is a constant; P_s is the saturation pressure of gas.

Generally, the traditional Langmuir and DR models have been verified at low pressures where the volume of the adsorbed phase is negligible. The term $(1 - \rho_g)/\rho_a$ is introduced into traditional models because the volume is occupied by the adsorbed phase on the sample surface rather than the free gas (Gensterblum et al. 2013; Sakurovs et al. 2008). However, because the term $(1 - \rho_g)/\rho_a$ is added, the Langmuir model has to be corrected when the density of the adsorbed phase is no longer negligible at high pressures. The DR model is only valid when the pressure is less than the saturation pressure of the gas ($P < P_s$). The modified models can be applied to high-pressure adsorption experiments, in particular with supercritical CO_2 by replacing P_L term using the Langmuir density (ρ_L), P_s using the adsorbed phase density (ρ_a) and P using the free gas density (ρ_g). The modified Langmuir and DR models are expressed as Eqs. 14 and 15, where the free parameters are n_0, ρ_L and D.

$$n_{ex} = n_0\left(1 - \rho_g/\rho_a\right)\left[\rho_g/\left(\rho_g + \rho_L\right)\right] \quad \text{(modified Langmuir model)} \tag{14}$$

$$n_{ex} = n_0\left(1 - \rho_g/\rho_a\right)\exp\left\{-D\left[\ln\left(\rho_a/\rho_g\right)\right]^2\right\} \quad \text{(modified DR model)} \tag{15}$$

where ρ_g is the free gas density; ρ_a is the adsorbed phase density; ρ_L is the Langmuir density when the amount of adsorption is half the maximum.

It was found that coal can adsorb gas on its surface and absorb gas into its interior (Larsen, 2004). A combination of modified Langmuir/DR and Henry equations are used to describe the two sorption mechanisms by coal, where the adsorption is expressed by the modified Langmuir or DR models, and the absorption by a term proportional to gas density, following Henry's law k. The term k collects errors in sample and cell volume, helium pycnometry density and adsorbed phase density. These refinements lead to the Eqs. 16 and 17, where the free parameters are n_0, ρ_L, D, and k.

$$n_{ex} = n_0\left(1 - \rho_g/\rho_a\right)\left[\rho_g/\left(\rho_g + \rho_L\right)\right] + k\rho_g \quad \text{(modified Langmuir + k model)} \tag{16}$$

$$n_{ex} = n_0\left(1 - \rho_g/\rho_a\right)\exp\left\{-D\left[\ln\left(\rho_a/\rho_g\right)\right]^2\right\} + k\rho_g \quad \text{(modified DR + k model)} \tag{17}$$

where k is the parameter related to the affinity of coal for fluid.

Figure 8 shows the fitting results of different models for 293.29 K and 352.57 K as examples. Figure 8a displays that the Langmuir + k equation provides a reasonable fitting result for liquid CO_2. Figure 8b displays that the DR + k equation has a better fitting result at 352.57 K. The prediction accuracy of each model can be represented by the average relative error (ARE) for the n data points.

$$ARE = \frac{1}{n}\sum_{1}^{n}\left|\frac{n_{ex,\exp} - n_{ex,cal}}{n_{ex,\exp}}\right| \times 100 \tag{18}$$

where $n_{ex,exp}$ and $n_{ex,cal}$ are the amount of the excess adsorption obtained from experiment and thermodynamic model fitting, respectively.

As indicated in Table 3, the Langmuir + k model has lowest ARE 4.50 % at 293.29 K, the DR + k model has the lowest ARE 2.48, 2.00 and 1.90 % at 311.11, 332.79 and 352.57 K, respectively. It suggests that the sorption mechanism tends to the monolayer adsorption when liquid CO_2 is adsorbing on coal, while the theory of pore filling is

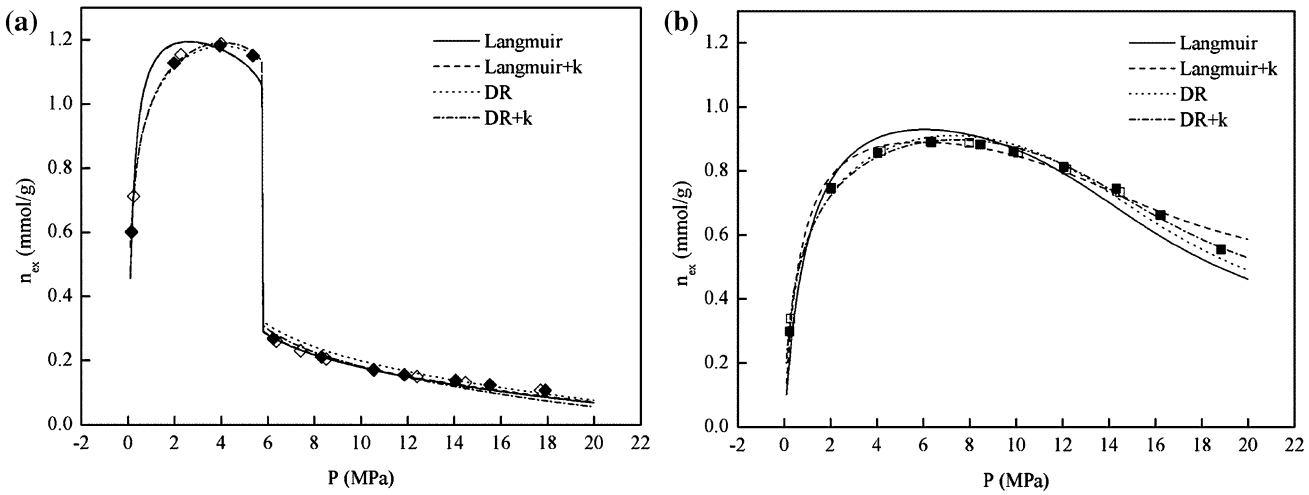

Fig. 8 Experimental data and thermodynamic models of the excess adsorption/desorption for CO_2 on dry coal, solid and open markers refer to adsorption and desorption, respectively. **a** 293.29 K; **b** 352.57 K

Table 3 Four models for CO_2 adsorption on dry coal at 293.29, 311.11, 332.79 and 352.57 K

T/K		Units	Langmuir	Langmuir + k	DR	DR + k
293.29	n_0	mmol/g	1.345	1.343	1.493	1.515
	ρ_L	g/cm^3	0.0035	0.0035	–	–
	k	cm^3/g	–	0.0028	–	−0.0241
	D	–	–	–	0.0245	0.0253
	ARE	%	4.64	4.50	7.42	6.68
311.11	n_0	mmol/g	1.302	1.275	1.422	1.441
	ρ_L	g/cm^3	0.0059	0.0055	–	–
	k	cm^3/g	–	0.0424	–	−0.0227
	D	–	–	–	0.0316	0.0324
	ARE	%	5.93	5.33	3.91	2.48
332.79	n_0	mmol/g	1.255	1.174	1.330	1.326
	ρ_L	g/cm^3	0.0113	0.0087	–	–
	k	cm^3/g	–	0.1310	–	0.0065
	D	–	–	–	0.0381	0.0379
	ARE	%	6.71	4.37	2.02	2.00
352.57	n_0	mmol/g	1.202	1.055	1.253	1.204
	ρ_L	g/cm^3	0.0162	0.0102	–	–
	k	cm^3/g	–	0.2963	–	0.0975
	D	–	–	–	0.0437	0.0410
	ARE	%	7.48	3.16	2.44	1.90

suitable for the supercritical CO_2. Table 3 also lists the fitting free parameters n_0, ρ_L, k and D of different models. It is revealed that there is a dependency between the temperature and free parameters. The fitted surface adsorption capacity n_0 decreases, yet ρ_L, D and k increase with the increasing temperature for the same model. Base on the meaning of the parameter k, the negative k values for DR + k model indicate that 0.0241 cm^3/g and 0.0227 cm^3/g of block coal sample are accessible to He but not access to CO_2 at 293.29 and 311.11 K, respectively. Besides, the increasing k value with temperature for anthracite could be due to improved access of the substrate by gas.

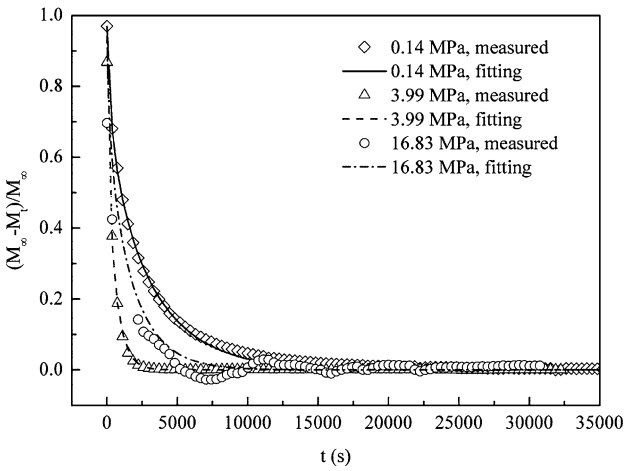

Fig. 9 Experimental and model fitting results of adsorption kinetics for CO_2 on dry coal at 311.11 K

3.5 Adsorption kinetics

The adsorption rates of CO_2 were monitored simultaneously with the isotherm test at each pressure. A total of 10 pressure experiments were conducted for each adsorption isotherm. The experimental data for the adsorption kinetics of CO_2 on dry coal are presented in Fig. 9 using 311.11 K as an example. The adsorption rate is represented using $(M_\infty - M_t)/M_\infty$. It can be observed from the figure that the kinetics data monotonically decrease with time, and the adsorption time to reach equilibrium at 3.99 MPa is shorter than the time at 0.14 MPa. In other words, the adsorption rate increases with the increasing pressure at low pressures. The results were also proven by Charrière et al. (2010) for (0.1 and 5) MPa at (283–333) K. However, the experimental data are fluctuant at the initial time range for high pressures due to the temperature variation in the adsorption cell after high-pressure CO_2 is injected.

3.6 Estimation of diffusivity from the modified unipore model

It is well-known that the diffusion plays an important role in the adsorption process. Consequently, many researchers apply diffusion model to estimate the diffusivity in the process of CO_2 adsorption on coal. However, the

Table 4 Estimated kinetic parameter C for CO_2 using the modified model at different pressures

	293.29 K		311.11 K		332.79 K		352.57 K	
	P (MPa)	C (s^{-1})	P (MPa)	C (s^{-1})	P (MPa)	C (s^{-1})	P (MPa)	C (s^{-1})
LP	0.15	3.35×10^{-4}	0.14	2.61×10^{-4}	0.16	3.04×10^{-4}	0.25	5.13×10^{-4}
	1.97	7.89×10^{-4}	2.04	9.10×10^{-4}	2.03	6.57×10^{-4}	2.02	8.29×10^{-4}
	3.94	1.09×10^{-3}	3.99	9.15×10^{-4}	4.15	9.17×10^{-4}	4.04	1.16×10^{-3}
HP	8.31	6.27×10^{-4}	8.10	1.06×10^{-3}	8.52	1.25×10^{-3}	8.45	9.67×10^{-4}
	11.86	1.38×10^{-3}	12.45	1.16×10^{-3}	12.85	6.40×10^{-4}	12.05	1.32×10^{-3}
	15.53	1.28×10^{-3}	16.83	5.10×10^{-4}	16.82	8.92×10^{-4}	16.21	9.55×10^{-4}
	17.90	2.11×10^{-3}	18.62	9.10×10^{-4}	18.50	7.81×10^{-4}	18.84	8.65×10^{-4}

conventional unipore and bidisperese models fail to predict the non-linear adsorption kinetics data at entire time range. According to Fick's second law, the solution of the diffusion equation for the spherical sorbent is given by the expression:

$$y = M_t/M_\infty = 1 - \left(6/\pi^2\right)\sum\left(1/n^2\right)\exp\left(-D'n^2\pi^2t/r^2\right) \quad (19)$$
$$n = 1, 2, 3, \ldots, \infty$$

where y is the fractional uptake ($0 \le y \le 1$); M_t is the total amount of CO_2 adsorbed at time t; M_∞ is the total amount of CO_2 adsorbed at infinite time; D' is the Fickian diffusion coefficient; r is the sphere radius, which is difficult to obtain for block coal sample, so D'/r^2 is often expressed as the effective diffusivity.

Because the solution of Eq. 19 would be different depending on the n value and the method used for the estimation. The kinetic parameter $C = \pi^2D'/r^2$ was introduced and Eq. 19 was modified as:

$$1 - y = 1 - M_t/M_\infty = \left(6/\pi^2\right)\sum\left(1/n^2\right)\exp\left(-n^2Ct\right)$$
$$n = 1, 2, 3, \ldots, \infty \quad (20)$$

where $C = \pi^2D'/r^2$ is a kinetic parameter and accounted for the effect of diffusion coefficient.

A simplified algorithm is proposed to estimate the parameter C with minimum error given, as shown in Eqs. 21 and 22 (Terzyk and Gauden 2001). Combined the simplified model and the modification of unipore model (Eq. 20) are applied to various pressure stages.

$$Ct = \pi^2D't/r^2 = f_1(y) = 0.286 \times 8.151^y \times y^{1.453} \quad (0.0025 \le y \le 0.8) \quad (21)$$

$$Ct = \pi^2D't/r^2 = f_2(y) = (0.285 - 0.284 \times y)/\left(1 - 1.927 \times y + 0.927 \times y^2\right) \quad (0.8 \le y \le 0.9) \quad (22)$$

In this study, the parameter C is assumed to be an average value for the whole diffusion process at each pressure, it does not change with time and concentration. The C value was determined for which both $f_1(y)/t$ and $f_2(y)/t$ yielded the same results, and used as an input to Eq. 20 for modeling the adsorption rate data. Additionally, the best value of n was checked for each pressure in this study, the results indicated that the best value of n was different for different pressures, but $n = 7$ was sufficient for estimation with satisfied accuracy for the experimental data using Eq. 20.

The kinetics parameter C was listed at two pressure ranges: low pressures (LP, 0.1 to 4.2 MPa) and high pressures (HP, greater than 4.2 MPa up to 18.9 MPa). It can be seen from Fig. 9 that the modified unipore model is able to predict the experimental kinetics data satisfactorily at 0.14 and 3.99 MPa. Due to the temperature variation at high pressures, the model cannot predict the fluctuant kinetics data well at the initial time range at 16.83 MPa. But the model can reflect the variation trend of the kinetics data with the stability of temperature. The values of kinetic parameter C for CO_2 at low and high pressures are calculated using Eqs. 21 and 22 which are shown in Table 4 for all temperatures. It can be seen from the table that C values increase with the increasing pressure at low pressures. The reason may be that the effect of pressure on the adsorption rate could be mainly controlled by both diffusion and adsorption of CO_2 into coal bulk. However, the influences of pressure on the C values are not obvious at high pressures, which is likely due to the variation in temperature for CO_2 diffusion. In addition, C values have no dependencies with temperature for CO_2, which agrees with the results of Li et al. (2010). Converting C value into effective diffusivity, the order of magnitude of diffusivity ranges from 10^{-5} s^{-1} to 10^{-4} s^{-1}, which is smaller than the result of Bhowmik and Dutta (2013) due to the different sizes of coal samples.

4 Conclusions

This paper investigates the adsorption behaviour of carbon dioxide on dry coal at 293.29, 311.11, 332.79, and 352.57 K and pressures up to 19 MPa via a gravimetric method. Four thermodynamic models are applied to fit the adsorption isotherms, and a modified unipore model is used to obtain the diffusivity. The following conclusions can be drawn from the study:

1. Adsorption characteristics of liquid and supercritical CO_2 on block coal were measured using the magnetic suspension balance. The results show that the adsorption and desorption process of CO_2 on coal is a physical adsorption. An inflection point of the excess adsorption isotherm appears when the phase transition pressure is reached for gas–liquid and gas-supercritical transition of CO_2.
2. Four isotherm models were used to analyse the adsorption behaviour of CO_2 on coal using CO_2 density instead of pressure. The sorption mechanism tends to the monolayer adsorption when liquid CO_2 is adsorbing on coal, while the theory of pore filling is suitable for the supercritical CO_2.
3. The adsorption kinetic experiments were conducted in a wide pressure range from 0.1 to 19 MPa. For low pressures, the amounts of excess adsorption increase monotonically with time and the adsorption rate increases with the increasing pressure. However, for high pressures, the experimental data are fluctuant at initial time range due to the temperature variation in the adsorption cell after high-pressure CO_2 is injected.
4. The modified unipore model was applied to CO_2 diffusion in the block coal. Simultaneously, the kinetic parameter C values were obtained from the modified model for CO_2. The C values increase with the increasing pressure at low pressures, but the influences of pressure on the C values are not obvious at high pressures. In addition, C values have no obvious dependencies with temperature.

Acknowledgments The authors thank the editor and the reviewers for the constructive comments that have helped to improve the quality of the paper. This work has been supported by the National Science and Technology Major Project of China (No. 2011ZX05026-004-07), the National Program on Key Basic Research Project (No. 2011CB707304) and the Fundamental Research Funds for the Central Universities.

Appendix

See Table 5.

Table 5 Experimental data of the excess adsorption and desorption for CO_2 on dry coal

Adsorption				Desorption			
P (MPa)	ρ (g/cm^3)	n_{ex} (mmol/g)	u_{nex} (mmol/g)	P (MPa)	ρ (g/cm^3)	n_{ex} (mmol/g)	u_{nex} (mmol/g)
293.29 K							
0.15	0.00263	0.60098	0.00000	17.90	0.92108	0.10755	0.00032
1.97	0.04004	1.12708	0.00001	17.70	0.91981	0.10762	0.00032
3.94	0.09468	1.18139	0.00003	14.47	0.89619	0.13142	0.00031
5.36	0.77996	0.26896	0.00006	12.40	0.87779	0.15037	0.00031
6.23	0.16042	1.15125	0.00027	10.55	0.85802	0.17118	0.00030
8.31	0.82680	0.21141	0.00029	8.51	0.82998	0.20518	0.00029
10.53	0.85787	0.17191	0.00030	7.40	0.80971	0.23141	0.00028
11.86	0.87243	0.15626	0.00030	6.36	0.78447	0.26109	0.00027
14.06	0.89278	0.13862	0.00031	3.99	0.09658	1.18799	0.00003
15.53	0.90438	0.12463	0.00032	2.28	0.04712	1.15343	0.00002
17.90	0.92108	0.10755	0.00032	0.24	0.00418	0.71246	0.00000
311.11 K							
0.14	0.00224	0.40587	0.00000	18.62	0.82342	0.21628	0.00029
2.04	0.03803	1.01185	0.00001	16.14	0.79331	0.25621	0.00028
3.99	0.08398	1.08330	0.00003	14.31	0.76446	0.29408	0.00027
6.23	0.16166	1.06401	0.00006	12.43	0.72368	0.35450	0.00025
8.10	0.31244	0.93870	0.00011	10.29	0.63648	0.50606	0.00022
9.89	0.64971	0.52164	0.00023	8.56	0.34879	0.88888	0.00012
12.45	0.74451	0.34048	0.00026	6.41	0.16555	1.04930	0.00006

Table 5 continued

Adsorption				Desorption			
P (MPa)	ρ (g/cm^3)	n_{ex} (mmol/g)	u_{nex} (mmol/g)	P (MPa)	ρ (g/cm^3)	n_{ex} (mmol/g)	u_{nex} (mmol/g)
14.24	0.77936	0.29284	0.00027	4.03	0.08389	1.07343	0.00003
16.83	0.80256	0.24252	0.00028	2.09	0.03876	1.00421	0.00001
18.62	0.82342	0.21628	0.00029	0.22	0.00352	0.51388	0.00000
332.79 K							
0.16	0.00246	0.30626	0.00001	18.50	0.68379	0.39644	0.00024
2.03	0.03469	0.86061	0.00001	15.90	0.61684	0.49901	0.00022
4.15	0.07767	0.95745	0.00003	14.24	0.55049	0.59803	0.00019
5.90	0.12115	0.97116	0.00004	12.37	0.43746	0.73234	0.00015
8.52	0.21081	0.93024	0.00007	11.16	0.35168	0.82215	0.00012
10.42	0.30388	0.85550	0.00011	7.96	0.18617	0.95545	0.00007
12.85	0.47102	0.69801	0.00016	6.00	0.12316	0.98068	0.00004
14.64	0.56883	0.56531	0.00020	3.97	0.07324	0.96402	0.00003
16.82	0.64382	0.45847	0.00022	2.06	0.03504	0.87068	0.00001
18.50	0.68379	0.39644	0.00024	0.32	0.00517	0.46300	0.00001
352.55 K							
0.25	0.00344	0.29914	0.00000	18.84	0.56674	0.55481	0.00020
2.02	0.03206	0.74423	0.00001	16.23	0.48017	0.66097	0.00017
4.04	0.06878	0.85566	0.00002	14.49	0.40733	0.73438	0.00014
6.36	0.11855	0.88951	0.00004	12.17	0.30539	0.80415	0.00011
8.45	0.17351	0.88252	0.00006	10.08	0.22513	0.85740	0.00008
9.90	0.21866	0.86111	0.00008	7.97	0.15983	0.88762	0.00006
12.05	0.30043	0.81205	0.00010	6.32	0.11774	0.89141	0.00004
14.32	0.39924	0.74462	0.00014	4.19	0.07166	0.86199	0.00003
16.21	0.47963	0.66253	0.00017	2.03	0.03219	0.74776	0.00001
18.84	0.56674	0.55481	0.00020	0.28	0.00413	0.33867	0.00000

References

Bae, J.S., Bhatia, S.K.: High-pressure adsorption of methane and carbon dioxide on coal. Energy Fuels **20**, 2599–2607 (2006)

Bhowmik, S., Dutta, P.: Adsorption rate characteristics of methane and CO_2 in coal samples from Raniganj and Jharia coalfields of India. Int. J. Coal Geol. **113**, 50–59 (2013)

Busch, A., Gensterblum, Y., Krooss, B.M., Littke, R.: Methane and carbon dioxide adsorption-diffusion experiments on coal: upscaling and modeling. Int. J. Coal Geol. **60**, 151–168 (2004)

Charrière, D., Pokryszka, Z., Behra, P.: Effect of pressure and temperature on diffusion of CO_2 and CH_4 into coal from the Lorraine basin (France). Int. J. Coal Geol. **81**, 373–380 (2010)

Clarkson, C.R., Bustin, R.M.: The effect of pore structure and gas pressure upon the transport properties of coal: a laboratory and modeling study. 1. Isotherms and pore volume distributions. Fuel **78**, 1333–1344 (1999a)

Clarkson, C.R., Bustin, R.M.: The effect of pore structure and gas pressure upon the transport properties of coal: a laboratory and modeling study. 2. Adsorption rate modeling. Fuel **78**, 1345–1362 (1999b)

Cui, X., Bustin, M.C., Dipple, G.: Selective transport of CO_2, CH_4 and N_2 in coals: insights from modeling of experimental gas adsorption data. Fuel **83**, 293–303 (2004)

Day, S., Fry, R., Sakurovs, R.: Swelling of Australian coals in supercritical CO_2. Int. J. Coal Geol. **74**, 41–52 (2008)

Dreisbach, F., Seif, A.H., Lösch, H.W.: Gravimetric measurement of adsorption gas mixture CO/H_2 with a magnetic suspension balance. Chem. Eng. Technol. **25**, 1060–1065 (2002)

Dutta, P., Harpalani, S., Prusty, B.: Modeling of CO_2 sorption on coal. Fuel **87**, 2023–2036 (2008)

Fang, Z., Li, X.: A preliminary evaluation of carbon dioxide storage capacity in unmineable coalbeds in China. Acta Geotech. **9**, 109–114 (2014)

Gensterblum, Y., van Hemert, P., Billemont, P., Battistutta, E., Busch, A., Krooss, B.M., Weireld, G.D., Wolf, K.H.A.A.: European inter-laboratory comparison of high pressure CO_2 sorption isotherms II: natural coals. Int. J. Coal Geol. **84**, 115–124 (2010)

Gensterblum, Y., Merkel, A., Busch, A., Krooss, B.M.: High-pressure CH_4 and CO_2 sorption isotherms as a function of coal maturity and the influence of moisture. Int. J. Coal Geol. **118**, 45–57 (2013)

Harpalani, S., Basanta, K.P., Dutta, P.: Methane/CO_2 sorption modeling for coalbed methane production and CO_2 sequestration. Energy Fuels **20**, 1591–1599 (2006)

Hol, S., Gensterblum, Y., Spiers, C.J.: Direct determination of total CO_2 uptake by coal: a new technique compared with the manometric method. Fuel **105**, 192–205 (2013)

Humayun, R., Tomasko, D.L.: High-resolution adsorption isotherms of supercritical carbon dioxide on activated carbon. AIChE J. **46**, 2065–2075 (2000)

Kelemen, S.R., Kwiatek, L.M.: Physical properties of selected block Argonne Premium bituminous coal related to CO_2, CH_4, and N_2 adsorption. Int. J. Coal Geol. **77**, 2–9 (2009)

Krooss, B.M., van Bergen, F., Gensterblum, Y., Siemons, N., Pagnier, H.J.M., David, P.: High-pressure methane and carbon dioxide adsorption on dry and moisture-equilibrated Pennsylvanian coals. Int. J. Coal Geol. **51**, 69–92 (2002)

Larsen, J.W.: The effects of dissolved CO_2 on coal structure and properties. Int. J. Coal Geol. **57**, 63–70 (2004)

Li, D., Liu, Q., Weniger, P., Gensterblum, Y., Busch, A., Krooss, B.M.: High-pressure sorption isotherms and sorption kinetics of CH_4 and CO_2 on coals. Fuel **89**, 569–580 (2010)

Majewska, Z., Ziętek, J.: Changes of acoustic emission and strain in hard coal during gas sorption-desorption cycles. Int. J. Coal Geol. **70**, 305–312 (2007)

Mianowski, A., Marecka, A.: The isokinetic effect as related to the activation energy for the gases diffusion in coal at ambient temperatures: part I. Fick's diffusion parameter estimated from kinetic curves. J. Therm. Anal. Calorim. **95**, 285–292 (2009)

Miknis, F.P., Netzel, D.A., Turner, T.F., Wallace, J.C., Butcher, C.H.: Effect of different drying methods on coal structure and reactivity toward liquefaction. Energy Fuels **10**, 631–640 (1996)

Mohammad, S., Fitzgerald, J., Robinson, R.L., Gasem, K.A.M.: Experimental uncertainties in volumetric methods for measuring equilibrium adsorption. Energy Fuels **23**, 2810–2820 (2009)

Nandi, S.P., Walker, P.L.: Activated diffusion of methane from coals at elevated pressures. Fuel **54**, 81–86 (1975)

Ottiger, S., Pini, R., Storti, G., Mazzotti, M., Bencini, R., Quattrocchi, F., Sardu, G., Deriu, G.: Adsorption of pure carbon dioxide and methane on dry coal from the Sulcis coal province (SW Sardinia, Italy). Environ. Prog. **25**, 355–364 (2006)

Ottiger, S., Pini, R., Storti, G., Mazzotti, M.: Competitive adsorption equilibria of CO_2 and CH_4 on a dry coal. Adsorption **14**, 539–556 (2008)

Ozdemir, E., Morsi, B.I., Schroeder, K.: Importance of volume effects to adsorption isotherms of carbon dioxide on coals. Langmuir **19**, 9764–9773 (2003)

Ozdemir, E., Morsi, B.I., Schroeder, K.: CO_2 adsorption capacity of Argonne premium coals. Fuel **83**, 1085–1094 (2004)

Pan, Z., Connell, L.D., Camilleri, M., Connelly, L.: Effects of matrix moisture on gas diffusion and flow in coal. Fuel **89**, 3207–3217 (2010)

Pini, R., Ottiger, S., Rajendran, A., Storti, G., Mazzotti, M.: Reliable measurement of near-critical adsorption by gravimetric method. Adsorption **12**, 393–403 (2006)

Romanov, V., Soong, Y.: Helium-volume dynamics of Upper Freeport coal powder and lumps. Int. J. Coal Geol. **77**, 10–15 (2009)

Sakurovs, R., Day, S., Weir, S., Duffy, G.: Application of a modified Dubinin-Radushkevich equation to adsorption of gases by coals under supercritical conditions. Energy Fuels **21**, 992–997 (2007)

Sakurovs, R., Day, S., Weir, S., Duffy, G.: Temperature dependence of sorption of gases by coals and charcoals. Int. J. Coal Geol. **73**, 250–258 (2008)

Sakurovs, R., Day, S., Weir, S.: Relationships between the critical properties of gases and their high pressure sorption behavior on coals. Energy Fuels **24**, 1781–1787 (2010)

Siemons, N., Busch, A.: Measurement and interpretation of supercritical CO_2 sorption on various coals. Int. J. Coal Geol. **69**, 229–242 (2007)

Siemons, N., Wolf, K.H.A.A., Bruining, J.: Interpretation of carbon dioxide diffusion behavior in coals. Int. J. Coal Geol. **72**, 315–324 (2007)

Song, Y., Jian, W., Zhang, Y., Shen, Y., Zhan, Y., Zhao, J., Liu, Y., Wang, D.: Densities and volumetric characteristics of binary system of CO_2 + Decane from (303.15 to 353.15) K and pressures up to 19 MPa. J. Chem. Eng. Data **57**, 3399–3407 (2012)

St. George, J.D., Barakat, M.A.: The change in effective stress associated with shrinkage from gas desorption in coal. Int. J. Coal Geol. **45**, 105–113 (2001)

Sudibandriyo, M., Pan, Z., Fitzgerald, J.E., Robinson, R.L., Gasem, K.A.M.: Adsorption of methane, nitrogen, carbon dioxide, and their binary mixtures on dry activated carbon at 318.2 K and pressures up to 13.6 MPa. Langmuir **9**, 5323–5331 (2003)

Terzyk, A.P., Gauden, P.A.: The simple procedure of the calculation of diffusion coefficient for adsorption on spherical and cylindrical adsorbent particles. Sep. Sci. Technol. **36**, 513–525 (2001)

Toribio, M.M., Oshima, Y., Shimada, S.: Evaluation of sequesterable carbon dioxide in Japanese coal samples at subcritical and supercritical conditions. Stud. Surf. Sci. Catal. **153**, 375–380 (2004)

van Hemert, P., Bruining, H., Rudolph, E.S.J., Wolf, K.H.A.A., Maas, J.G.: Improved manometric setup for the accurate determination of supercritical carbon dioxide sorption. Rev. Sci. Instrum. (2009). doi:10.1063/1.3063064

Zhang, Y., Chang, F., Song, Y., Zhao, J., Zhan, Y., Jian, W.: Density of carbon dioxide + brine solution from Tianjin reservoir under sequestration conditions. J. Chem. Eng. Data **56**, 565–573 (2011)